

# Rac1 accumulates in the nucleus during the G2 phase of the cell cycle and promotes cell division

David Michaelson,<sup>2,5</sup> Wasif Abidi,<sup>2,5</sup> Daniele Guardavaccaro,<sup>4,5</sup> Mo Zhou,<sup>3,5</sup> Ian Ahearn,<sup>3,5</sup> Michele Pagano,<sup>4,5</sup> and Mark R. Philips<sup>1,2,3,5</sup>

<sup>1</sup>Department of Medicine, <sup>2</sup>Department of Cell Biology, <sup>3</sup>Department of Pharmacology, <sup>4</sup>Department of Pathology, and the <sup>5</sup>New York University Cancer Institute, New York University School of Medicine, New York, NY 10016

**R**ac1 regulates a wide variety of cellular processes. The polybasic region of the Rac1 C terminus functions both as a plasma membrane-targeting motif and a nuclear localization sequence (NLS). We show that a triproline N-terminal to the polybasic region contributes to the NLS, which is cryptic in the sense that it is strongly inhibited by geranylgeranylation of the adjacent cysteine. Subcellular fractionation demonstrated endogenous Rac1 in the nucleus and Triton X-114 partition revealed that this pool is prenylated. Cell cycle-blocking agents, synchroni-

zation of cells stably expressing low levels of GFP-Rac1, and time-lapse microscopy of asynchronous cells revealed Rac1 accumulation in the nucleus in late G2 and exclusion in early G1. Although constitutively active Rac1 restricted to the cytoplasm inhibited cell division, activated Rac1 expressed constitutively in the nucleus increased the mitotic rate. These results show that Rac1 cycles in and out of the nucleus during the cell cycle and thereby plays a role in promoting cell division.

## Introduction

Rac1 is among the most extensively characterized members of the Rho family of small GTPases. Like all GTPases, Rac1 functions as a molecular switch regulated by GTP/GDP exchange. Rac1 regulates a wide variety of cellular functions including actin remodeling for cell ruffling, adherens junction formation, cell motility, and polarity. Other functions of Rac1 include transcriptional activation and regulation of the NADPH oxidase (Jaffe and Hall, 2005). Rac1 has also been implicated in cellular transformation and may promote cell cycle progression through induction of cyclin D1 (Westwick et al., 1997).

Rac1 is regulated by numerous guanine nucleotide exchange factors (GEFs) and several GTPase-activating proteins (GAPs) and signals by interacting with a large set of effectors (Jaffe and Hall, 2005). The specificities of the several GEFs and GAPs and numerous effectors that interact with Rac1 may explain its myriad functions. However, differential regulation of signaling by Rac1 in different contexts is poorly understood. Increasing evidence suggests that subcellular localization plays

a major role in regulating the signaling output of promiscuous regulatory proteins such as Rac1 (Mor and Philips, 2006).

Like all Rho proteins, Rac1 is targeted within cells by posttranslational modification of a C-terminal CAAX motif by prenylation, proteolysis, and carboxyl methylation and by association with a cytosolic chaperone, Rho guanosine nucleotide dissociation inhibitor (RhoGDI; Michaelson et al., 2001). In resting cells, Rac1 is found in the cytosol as a soluble 1:1 complex with RhoGDI. Upon activation, Rac1 is discharged from RhoGDI and displays affinity for the plasma membrane (Michaelson et al., 2001). This affinity can be explained by the geranylgeranyl modification of the Rac1 C terminus that functions in conjunction with a strong polybasic region immediately adjacent to the prenylcysteine (Michaelson et al., 2001). In its plasma membrane-binding capacity, Rac1 behaves like K-Ras4B, which also has a strong polybasic region. The polybasic region binds via electrostatic interactions with the negatively charged inner leaflet of the plasma membrane (Yeung et al., 2006). Recently, we have shown that the plasma membrane localization of Rac1 is modulated during phagocytosis by loss of the negative charge on the inner leaflet of the membrane (Yeung et al., 2006).

In addition to the cytosol and plasma membrane, GFP-Rac1 has been localized to the nuclear envelope (Kraynov et al., 2000; Michaelson et al., 2001) and nucleoplasm (Michaelson et al., 2001;

D. Michaelson and W. Abidi contributed equally to this paper.

Correspondence to M.R. Philips: philim01@med.nyu.edu

Abbreviations used in this paper: GAP, GTPase-activating protein; GEF, guanine nucleotide exchange factor; IF, immunofluorescent; NLS, nuclear localization sequence; PAE, porcine aortic endothelial; RhoGDI, Rho guanosine nucleotide dissociation inhibitor.

The online version of this paper contains supplemental material.

© 2008 Michaelson et al.

The Rockefeller University Press \$30.00

J. Cell Biol. Vol. 181 No. 3 485–496

www.jcb.org/cgi/doi/10.1083/jcb.200801047

Supplemental Material can be found at:  
<http://www.jcb.org/cgi/content/full/jcb.200801047/DC1>

Lanning et al., 2003). Lanning et al., (2003, 2004) identified the polybasic sequence of the Rac1 hypervariable region as a nuclear localization sequence (NLS), raising the question of how a single motif can target a protein to two distinct compartments, the plasma membrane and the nucleus. These investigators also found that the NLS of Rac1 was partially responsible for the accumulation in the nucleus of the armadillo repeat proteins smgGDS and p120 catenin (Lanning et al., 2003) and was required for efficient proteosomal degradation of Rac1 (Lanning et al., 2004). In these studies, a constitutively GTP-bound form of Rac1 was slightly more efficient in nuclear entry (Lanning et al., 2003, 2004). Rac1, in association with MgcRacGAP, has also been implicated in the nuclear import of STAT5 (Kawashima et al., 2006). Spatiotemporal studies of Rac1 activation in live cells using fluorescence resonance energy transfer (FRET)-based biosensors have revealed conflicting results with regard to the activation state of nuclear Rac1. Kravynov et al., (2000) found a large pool of GFP-Rac1 in the nucleoplasm that remained inactive. In contrast, Wong and Isberg (2005) detected active GFP-Rac1 in the nucleus but only in cells infected with *Yersinia* strains that secrete YopT, a prenylcysteine endoprotease that relocated Rac1 to the nucleus. Yoshizaki et al., (2003) used an intramolecular FRET probe that assesses the balance of GEFs and GAPs for Rac1 in cells undergoing mitosis and found that the balance favored inactive Rac1 in the region of the mitotic spindle.

We have studied the structure and regulation of the Rac1 NLS and the basis for the seemingly stochastic nature of its engagement. We show for the first time that a pool of endogenous Rac1 is nuclear. We find that a triproline motif adjacent to the polybasic sequence contributes to the NLS and that the NLS is cryptic in the sense that it is inhibited by the adjacent geranylgeranyl modification. Despite the inhibitory effect of prenylation on the NLS, we found that endogenous nuclear Rac1 is lipidated. We found that the distinct populations of cells with and without nuclear expression of Rac1 could be explained by a cell cycle dependence on nuclear import: Rac1 accumulated in the nucleus in late G2 and was excluded from this compartment in early G1. Although nuclear-targeted GTP-bound Rac1 accelerated cell division, GTP-bound Rac1 restricted to the cytoplasm had the opposite effect. Thus, Rac1 cycles in and out of the nucleus and thereby plays a role in cell division.

## Results

### Rac1 has a strong C-terminal NLS inhibited by prenylation

To better define the NLS at the C terminus of Rac1, we studied the subcellular localization of GFP extended with full-length Rac1, mutants thereof, or isolated C-terminal sequences of various lengths (Fig. 1 A). GFP alone and small GFP fusion proteins are well known to accumulate in the nucleoplasm as well as the cytoplasm. However, the pattern of nuclear GFP-Rac1 could be easily distinguished from that of GFP alone in most cell types by a much higher degree of contrast between the nuclear and cytoplasmic fluorescence (Fig. 1 B). Because the extent of nuclear localization appeared to depend on cell

type, we studied the distribution of these proteins in multiple cell lines including MDCK, COS-1, and porcine aortic endothelial (PAE) cells (Fig. 1, B and C) and ECV304 human bladder carcinoma, HeLa, and NIH 3T3 (not depicted). GFP-Rac1 ranged from  $5 \pm 2\%$  nuclear in MDCK cells to  $30 \pm 5\%$  nuclear in COS-1 cells (Fig. 1 C). Constitutively GTP-bound GFP-Rac1L61 was distributed in a pattern similar to that of wild-type GFP-Rac1 in each of the cell types. Moreover, GFP extended with the 11 C-terminal amino acids of Rac1 showed a higher degree of nuclear localization relative to the full-length protein in all cell lines studied. These observations suggest that the polybasic 11-amino acid C-terminal sequence contains an NLS and that the GTP-binding state of the molecule does not affect the NLS.

Because the canonical NLS of the polyomavirus large T antigen begins with a diproline, we sought to determine if the unusual triproline motif immediately upstream of the polybasic region in the Rac1 C terminus contributes to the NLS. GFP extended with the C-terminal 21 amino acids of Rac1 that included the triproline sequence was significantly more nuclear than either GFP extended with the 11-amino acid tail or full-length Rac1 in all cell types (Fig. 1 C). Indeed, in PAE cells, this construct was nuclear in  $80 \pm 5\%$  of cells. In contrast, when a 21-amino acid tail was used in which the triproline motif was mutated to trialanine, the sequence was no more potent in directing GFP into the nucleus than was the 11-amino acid tail. Thus, the triproline motif immediately N-terminal to the polybasic sequence contributes significantly to the NLS of Rac1. Neither GFP-Rac2 nor GFP-Rac3 was observed in the nucleus (Michaelson et al., 2001; Chan et al., 2005). The former has a PQP motif upstream of the polybasic region and the latter retains the same triproline sequence as Rac1. However, both have weak polybasic sequences relative to that of Rac1. Substitution of the K-Ras4B polybasic region (KKKKKKSKTK) for that of Rac1 (VKKRKRK) did not reconstitute the NLS, despite retention of the triproline sequence (Fig. 1 D). Thus, a polyproline sequence does not confer NLS activity upon all polybasic sequences and there appears to be specificity in the polybasic sequence of Rac1 that is preceded by a hydrophobic valine and has a net charge of +6.

Most striking was the nuclear localization of GFP-Rac1 that could not be prenylated because the CAAX cysteine was mutated to serine (SAAX mutant). Whether in a wild-type or constitutively active background, these constructs were virtually entirely nuclear such that under fluorescence microscopy, the nuclei were the only structures apparent (Fig. 1 B). GFP-tagged Rac1 with a three-amino acid C-terminal truncation (GFP-Rac1 $\Delta$ AAX) that, like the SAAX mutant, cannot be posttranslationally processed, also displayed a nuclear-only pattern (see Fig. 8 B). These observations suggest that the NLS of Rac1 is intrinsically as strong as that of nuclear proteins such as SV40 large T antigen but is weakened by prenylation. This conclusion is concordant with the results of Wong and Isberg (2005), who found GFP-Rac1 in the nucleus of cells infected with *Yersinia* strains that produce YopT, an endoprotease that removes prenylcysteine residues. To confirm that prenylation inhibits the NLS, we determined the effect of compactin

**A**

GFP-Rac1-AIRAVLCPPPVKKRKRKCLLL	Wt	(Geranylgeranylated)
GFP-Rac1L61-AIRAVLCPPPVKKRKRKCLLL	L61	(GTP-bound)
GFP-Rac1-AIRAVLCPPPVKKRKRKCVLS	CVLS	(Farnesylated)
GFP-Rac1-AIRAVLCPPPVKKRKRKSLLL	SAAX	(Unprenylated)
GFP-Rac1-AIRAVLCPPPVKKRKRKC	ΔAAX	(Unprenylated)
GFP-AIRAVLCPPPVKKRKRKCLLL	21aa Tail	
GFP-AIRAVLCAAAVKKRKRKCLLL	21aa 3P→3A Tail	
GFP-VKKRKRKCLLL	11aa Tail	
GFP-Rac1-AIRAVLCPPPKKKKKSKTKCVIM	Rac1/Ktail	

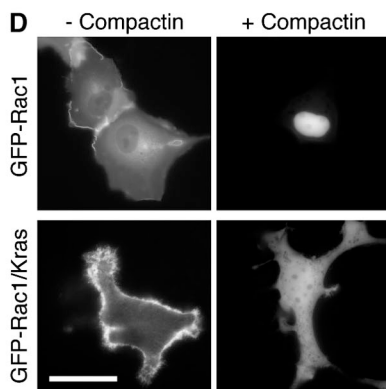
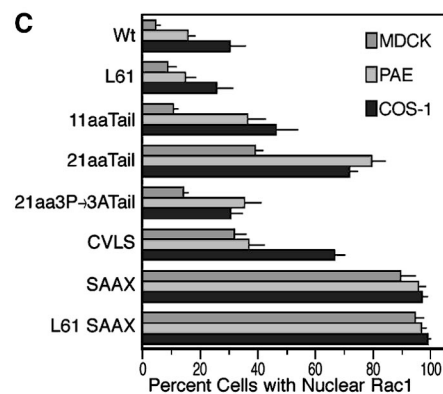
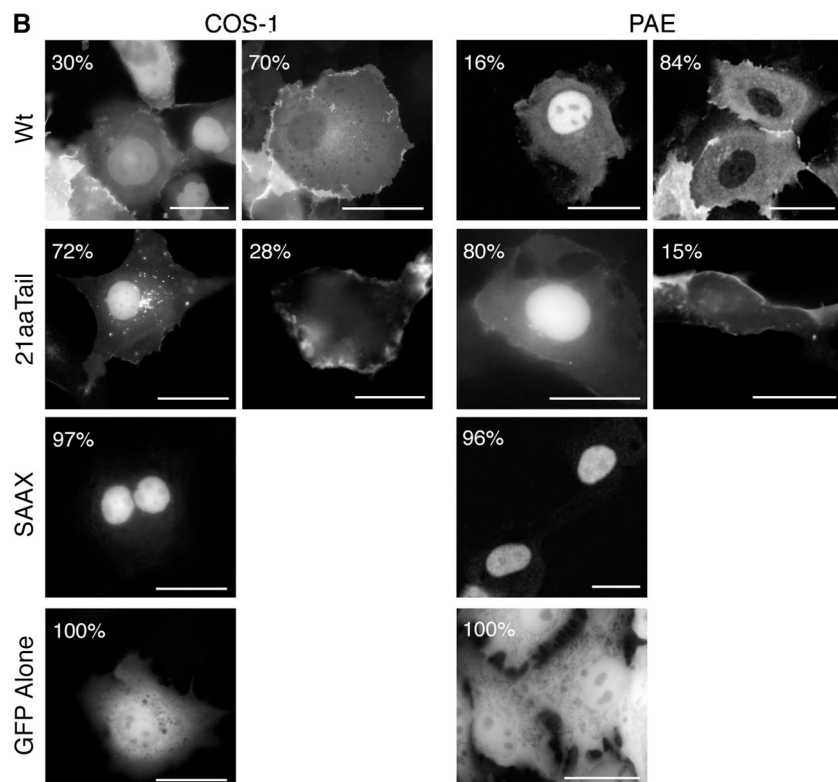
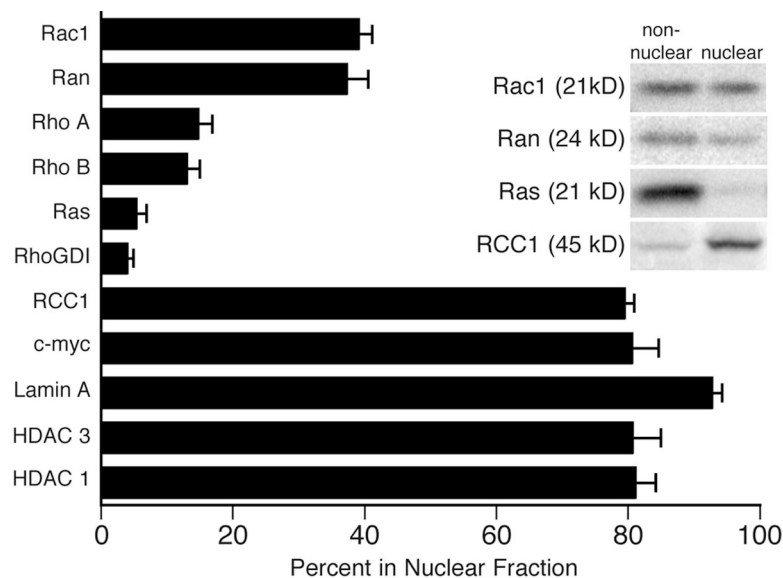


**Figure 1. The Rac1 NLS consists of the polybasic region in the C terminus, is strengthened by a flanking triproline motif, and is inhibited by geranylgeranylation.** (A) Description of constructs used. (B) Representative distribution patterns of the GFP-tagged constructs in live COS-1 and PAE cells with the percentage of cells showing the represented phenotype indicated. (C) Percentage of cells showing nuclear fluorescence greater than cytoplasmic fluorescence for the indicated constructs in MDCK, PAE, and COS-1 cells (mean  $\pm$  SEM;  $n \geq 4$ ). (D) Distribution of fluorescence in COS-1 cells expressing GFP-Rac1 or GFP-Rac1/Ktail with or without treatment with 10  $\mu$ M compactin. Only the nucleus is visible in cells expressing GFP-Rac1 treated with compactin. Bars, 10  $\mu$ m.

on nuclear localization of Rac1. This agent is an HMG-CoA reductase inhibitor that blocks prenylation by reducing the availability of farnesyl and geranylgeranyl pyrophosphates. GFP-Rac1 was entirely nuclear in cells treated with compactin (Fig. 1 D). As a control, we studied the effect of compactin on a chimeric protein consisting of GFP followed by the first 181 amino acids of Rac1 that precede the polybasic region, followed by the 14-amino acid polybasic region of K-Ras4B (GFP-Rac1K-tail). This construct was localized, like GFP-K-Ras4B, to the

plasma membrane of untreated cells. The chimera was mislocalized in cells treated with compactin in a fashion identical to that of GFP-K-Ras4B. Rather than accumulating exclusively in the nucleus like GFP-Rac1, the chimera was distributed in a homogeneous pattern in the cytosol and nucleoplasm (Fig. 1 D) indistinguishable from the pattern of GFP alone (Fig. 1 B). This demonstrates that the Rac1 polybasic region is distinct from that of K-Ras4B in functioning as a strong NLS that is inhibited by prenylation.

**Figure 2. Endogenous Rac1 is in the nucleus.** COS-1 cells were separated into nuclear and nonnuclear fractions as described in Materials and methods. Equal cell equivalents of each fraction were analyzed by SDS-PAGE and immunoblots (inset) for the indicated proteins. Immunoprecipitated proteins were detected and quantified with [ $^{125}$ I]protein A and phosphorimaging, and the percentage of total protein in the nuclear fraction was calculated (mean  $\pm$  SEM;  $n = 3$ ).



One explanation for prenylation-dependent exclusion of Rac1 from the nucleus is that binding to its cytosolic chaperone RhoGDI, a process known to be prenylation-dependent (Michaelson et al., 2001), blocks the NLS. However, because the 11- and 21-amino acid tail constructs that cannot bind RhoGDI were only partially nuclear, RhoGDI cannot be the only mechanism of inhibiting the NLS. To test the idea that the inhibitory effect of the geranylgeranyl group on the NLS was related to its hydrophobicity, we studied GFP-Rac1-CVLS in which the native CAAX motif (CLLL) was substituted for CVLS, which directs modification by a 15-carbon farnesyl isoprenoid rather than a 20-carbon geranylgeranyl lipid. We have previously shown that farnesylation rather than geranylgeranylation of Rac1 does not affect binding to RhoGDI (Michaelson et al., 2001). GFP-Rac1-CVLS was observed to be nuclear in each cell line with twice the frequency as that of GFP-Rac1 (Fig. 1 C). This suggests that the hydrophobicity of the prenyl modification inhibits the action of the NLS. Collectively, our data reveal that the polybasic region of the Rac1 C terminus in conjunction with the triproline motif immediately adjacent provides a strong NLS that is cryptic in that it is inhibited by prenylation of the CAAX cysteine. This reveals a new role for geranylgeranylation of Rac1: in addition to providing a membrane anchor and mediating RhoGDI binding, the lipid modification also blocks a strong NLS.

#### Endogenous Rac1 is in the nucleus

To date, only overexpressed, epitope-tagged Rac1 has been observed in the nucleus. To determine if endogenous Rac1 is localized in the nucleus, we performed indirect immunofluorescent (IF) staining. However, we were unsuccessful because we could not find a suitable anti-Rac1 antibody. We tried three commercially available anti-Rac1 antibodies each with three fixation/permeabilization methods (paraformaldehyde/Triton X-100, paraformaldehyde/saponin, and methanol/acetone) on each of five cell types (COS-1, MDCK, NIH 3T3, PAE, and HeLa). We found a wide variety of fluorescence staining patterns, including those that clearly showed prominent nuclear staining

(Fig. S1 A, available at <http://www.jcb.org/cgi/content/full/jcb.200801047/DC1>). Unlike GFP-Rac1 expression, which was nuclear in a subset of transfected cells, when anti-Rac1 antibodies revealed nuclear staining, they did so for the entire population of cells. This incongruity and the overall variability of the assay raised doubts about the specificity of the antibodies. We therefore performed IF staining with each anti-Rac1 antibody on mouse embryonic fibroblasts from mice homozygous for a floxed *Rac1* allele (Walmsley et al., 2003). We stained cells after infection with an adenovirus directing expression of Cre recombinase or  $\beta$ -galactosidase. Immunoblots revealed that Rac1 expression was completely lost in cells infected with adeno-Cre (Fig. S1 B). The IF staining pattern was identical in cells with or without Rac1 (Fig. S1 C). We conclude that none of the commercially available antibodies reliably reports the subcellular localization of endogenous Rac1 in fixed cells.

Because the antibodies that proved unreliable in IF staining are unequivocally specific in immunoblots, we turned to subcellular fractionation to determine if there is a nuclear pool of endogenous Rac1. The nuclei and nonnuclear compartments of COS-1 were separated by standard methods and each fraction was analyzed for Rac1 and control proteins by immunoblots quantified using [ $^{125}$ I]protein A and phosphorimaging (Fig. 2). Ras and RhoGDI were detected almost exclusively in the non-nuclear fraction and >80% of RhoA and RhoB were also detected in this fraction. In contrast, >80% of each of five known nuclear proteins was detected in the nuclear fraction. 40% of Ran, a non-CAAX GTPase that shuttles in and out of the nucleus via nuclear importins, was detected in the nuclear fraction of subconfluent cells. Rac1 had a profile similar to Ran, with recoveries of  $39 \pm 3\%$  in the nuclear fraction. Similar results were obtained for NIH 3T3 and PAE cells (unpublished data). We conclude that a portion of endogenous Rac1 is nuclear.

#### Endogenous Rac1 in the nucleus is prenylated

Our observation that geranylgeranylation inhibits the NLS of Rac1 suggested that the nuclear pool of Rac1 may not be prenylated.

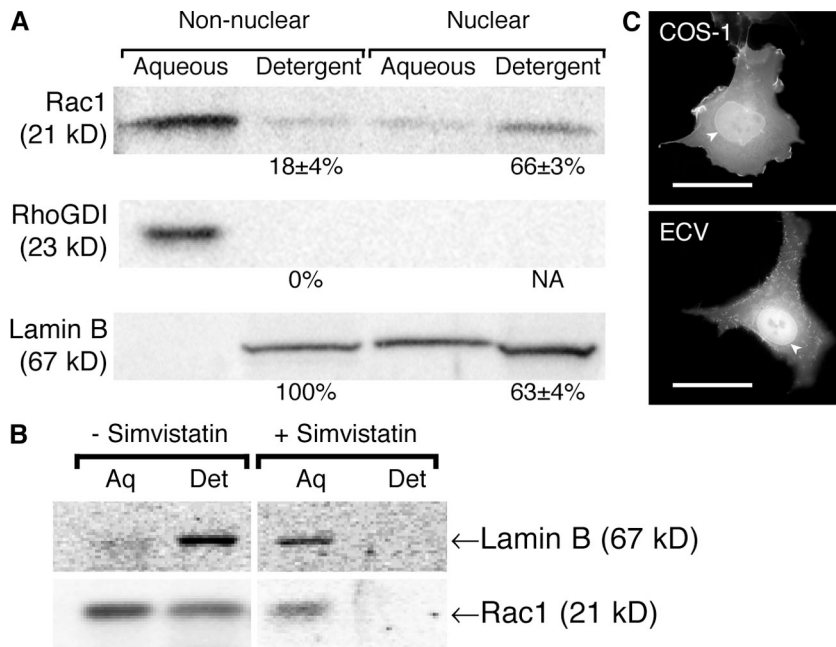


**Figure 3. Nuclear Rac1 is prenylated.** (A) Nuclear and nonnuclear fractions were prepared as described in Materials and methods. After separation, each fraction was brought to 1% Triton X-114 and phase separation was initiated by heating the samples to 37°C. The aqueous and detergent phases of each fraction were analyzed for Rac1, RhoGDI, and lamin B by immunoblotting. Immunoblots were quantified with [<sup>125</sup>I]protein A and phosphorimaging, and the percentage of total protein in each fraction in the detergent phase was calculated (mean ± SEM; n = 3). (B) Triton X-114 partition as shown in A was performed on the nuclear fractions of COS-1 cells treated overnight with or without 10 μM simvastatin. Aq, aqueous; Det, detergent phases. (C) Selected images of GFP-Rac1 in COS-1 and ECV cells showing prominent decoration of the nuclear envelope (arrowhead). Bars, 10 μm.

To test this, we performed Triton-X 114 partition analysis on the nuclear and nonnuclear pools of Rac1. This method relies on the temperature-dependent separation of the nonionic detergent into aqueous and detergent phases. Prenylated proteins without lipid sequestering chaperones partition into the detergent phase (Hancock, 1995). Prenylated proteins associated with chaperones that sequester the prenyl group would be expected to partition into the aqueous phase. More than 80% of endogenous Rac1 from the nonnuclear fraction partitioned into the aqueous phase, which is consistent with the 1:1 binding of Rac1 and RhoGDI that we described previously (Michaelson et al., 2001). Lamin B, a farnesylated protein without a known prenyl-binding chaperone that is synthesized and prenylated in the cytosol and then transported into the nucleus, served as a control. RhoGDI, a hydrophilic protein excluded from the nucleus, was an additional control. Although RhoGDI was entirely aqueous in the nonnuclear fraction, lamin B was found entirely in the detergent phase in this fraction, demonstrating that the pool of nascent lamin B awaiting nuclear import was fully lipidated, which is consistent with the idea that prenylation is exceedingly efficient. As expected, RhoGDI could not be detected in the nuclear fraction. In the nuclear fraction, 63 ± 4% of lamin B partitioned into the detergent phase, indicating that either some nuclear lamin B is delipidated, perhaps through proteolysis, or that Triton X-114 partition is not as efficient from the nuclear fraction that contains viscous chromatin than it is from the aqueous cytosol. Nuclear, endogenous Rac1 behaved like lamin B, with 66 ± 3% partitioning into the detergent phase (Fig. 3 A). Both Rac1 and lamin B were shifted into the aqueous phase in nuclei from cells treated with simvastatin, a potent HMG-CoA reductase inhibitor (Fig. 3 B). We conclude that, contrary to our expectation, a significant portion of nuclear Rac1 is prenylated.

A subset of cells expressing nuclear GFP-Rac1 revealed decoration of the nuclear envelope in addition to expression in

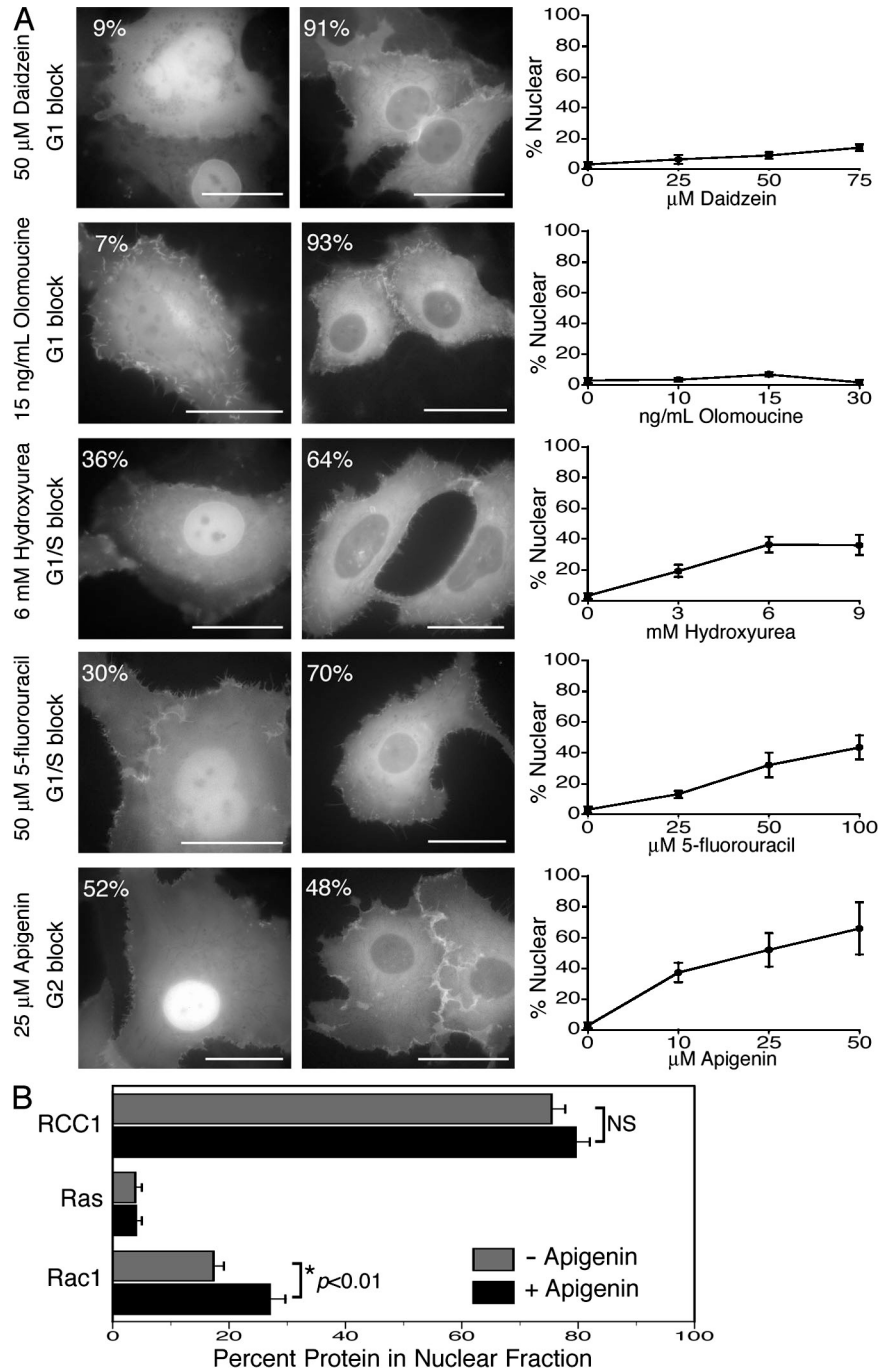
the nucleoplasm. GFP-Rac1 in the nuclear envelope gave a pattern that was smooth, continuous and relatively thick (Fig. 3 C). This is the same pattern that has been reported for GFP-lamin B (Kitten and Nigg, 1991), a farnesylated protein known to associate with the inner nuclear envelope. This suggests that the portion of the nuclear Rac1 that associates with the inner nuclear envelope does so by retention of the geranylgeranyl modification during nuclear import.

#### Rac1 accumulates in the nucleus during G2

The stochastic nature of the expression of GFP-Rac1 in the nucleoplasm and nuclear envelope in individual cells (Fig. 1 A) suggested that nuclear entry might be regulated by the cell cycle. To test this idea, we studied PAE cells stably expressing GFP-Rac1 at levels below endogenous (Fig. S2, available at <http://www.jcb.org/cgi/content/full/jcb.200801047/DC1>) and used several agents known to arrest cultured cells at various stages of the cell cycle (Fig. 4 A). Hydroxyurea and 5-fluorouracil, agents that promote G1/S arrest, both increased the percentage of cells with nuclear Rac1 from 20% to 36% and 30%, respectively. The agent that had the most dramatic effect, increasing cells with nuclear Rac1 to 52%, was apigenin, a compound that promotes G2 arrest by inducing p53 (Plaumann et al., 1996). In contrast, daidzein and olomoucine, agents that promote G1 arrest, had no effect. Similar results were obtained with ECV304 and NIH 3T3 cells stably expressing GFP-Rac1. To determine if apigenin could cause nuclear accumulation of endogenous Rac1, we performed subcellular fractionation on untransfected PAE cells exposed to this agent or a vehicle control. Although the portion in the nuclear fraction of Ras (a non-nuclear control) and RCC1 (a nuclear control) was not changed by apigenin treatment, the portion of Rac1 in the nuclear fraction increased by 55% (Fig. 4 B).

To determine the cell cycle dependence of nuclear Rac1 in cycling cells, we studied PAE cells stably expressing low levels

**Figure 4. The effect of cell cycle blockade on the nuclear expression of GFP-Rac1 and endogenous Rac1.** (A) PAE cells stably expressing GFP-Rac1 at levels below endogenous Rac1 (Fig. S1, available at <http://www.jcb.org/cgi/content/full/jcb.200801047/DC1>) were scored for the percentage of cells showing strong nuclear fluorescence before and 16 h after the addition of increasing amounts of the indicated compounds. Representative cells at the indicated dose are shown with the percentage of cells showing each phenotype indicated (left), and cumulative dose-response data are shown on the right (mean  $\pm$  SEM;  $n = 3$ ). Bars, 10  $\mu$ m. (B) Endogenous Rac1, Ras, and RCC1 were measured in the nuclear fractions as described in Fig. 2 before and after the addition of 50  $\mu$ M apigenin for 24 h (mean  $\pm$  SEM;  $n = 4$ ).



of GFP-Rac1 that were synchronized in G1/S by serum starvation and treatment with hydroxyurea and then released from the block. The percentage of cells with nuclear Rac1 was determined as these cells progressed through the cell cycle (Fig. 5 A). The highest levels of nuclear Rac1 were observed 8 h after release from the block, when the highest proportion of cells (75%) were observed to be in G2 by propidium iodide cytofluorimetry (Fig. 5 B). Cyclin A accumulates in the nucleus of cells in S and G2 phase. We therefore stained for cyclin A a population of unsynchronized COS-1 cells expressing GFP-Rac1. Although 93% of transfected cells expressing GFP-Rac1 in the nucleus stained for cyclin A, only 13% of cells with GFP-Rac1 excluded from the nucleus stained for this marker (Fig. 5 C). Similar re-

sults were obtained with PAE cells expressing GFP-Rac1 below endogenous levels (unpublished data). The results of the release from hydroxyurea block and cyclin A staining together with those using agents that promote cell cycle arrest indicate that Rac1 accumulates in the nucleus in G2.

The appearance of cyclin A in the nucleus during G2 is mediated by an increase in the level of expression of this protein. To determine if Rac1 expression levels fluctuate during the cell cycle, we analyzed a population of synchronized T98G cells by immunoblotting (Dorrello et al., 2006). We first confirmed that T98G cells behaved like the other cell lines we examined in showing GFP-Rac1 in the nucleus of a subset of unsynchronized cells (Fig. 6 A). As expected, levels of cyclins A

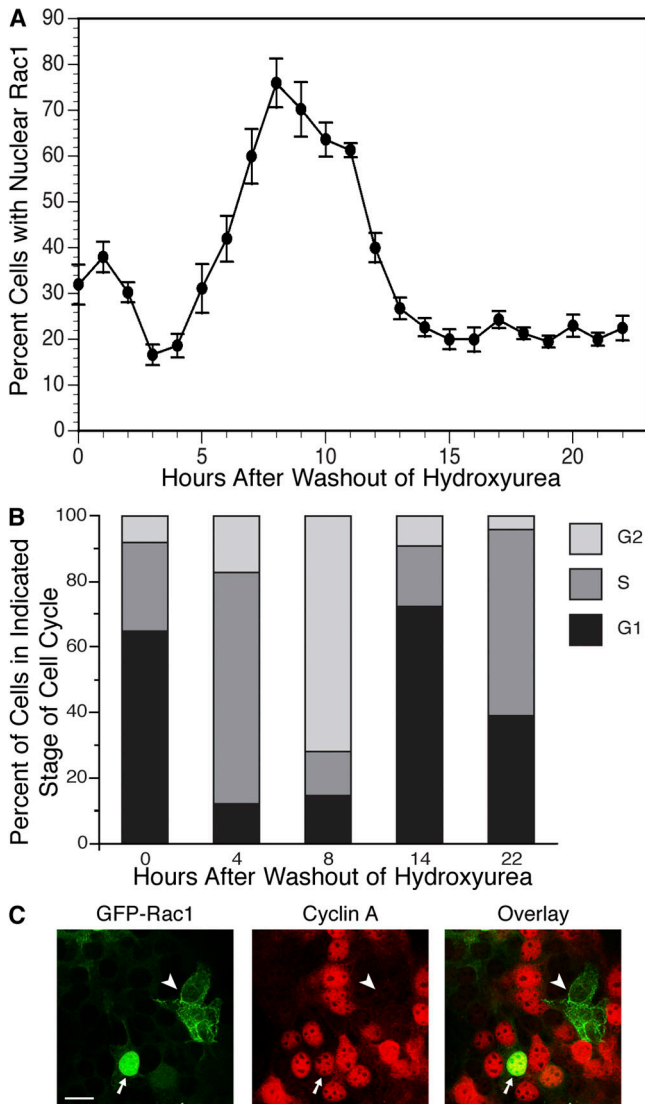


**Figure 5. Expression of Rac1 in the nucleus peaks in G2.** (A) PAE cells stably expressing GFP-Rac1 at levels below endogenous were synchronized in G1/S by serum starvation followed by hydroxyurea and then released. The percentage of cells with nuclear Rac1 was determined hourly and plotted as mean  $\pm$  SEM ( $n = 4$ ). (B) Aliquots of the cells analyzed in A were scraped from plates at the indicated times and analyzed for stage of the cell cycle by propidium iodide and cytofluorimetry. (C) Unsynchronized COS-1 cells were transfected with GFP-Rac1 and, after 16 h, fixed and stained for cyclin A, a marker of G2/M, those excluding the protein from the nucleus (arrowheads) did not. This correlation held for 93% of transfected cells examined ( $>100$ ). Bars, 10  $\mu$ m.

and D1 fluctuated in synchronized cells progressing through the cell cycle (Fig. 6 B). In contrast, the levels of Rac1, like those of ERK1 and ERK2, remained constant, indicating that the fluctuation of Rac1 in the nucleus represents redistribution rather than oscillations in its expression. These results were confirmed in IMR-90 diploid primary human fibroblasts (Sherwood et al., 1988) that are wild type at both the Rb and p53 loci (Fig. 6 C).

To confirm the cell cycle dependence of nuclear Rac1 in dividing cells untreated with drugs, we studied by time-lapse fluorescent microscopy PAE and NIH3T3 cells stably expressing

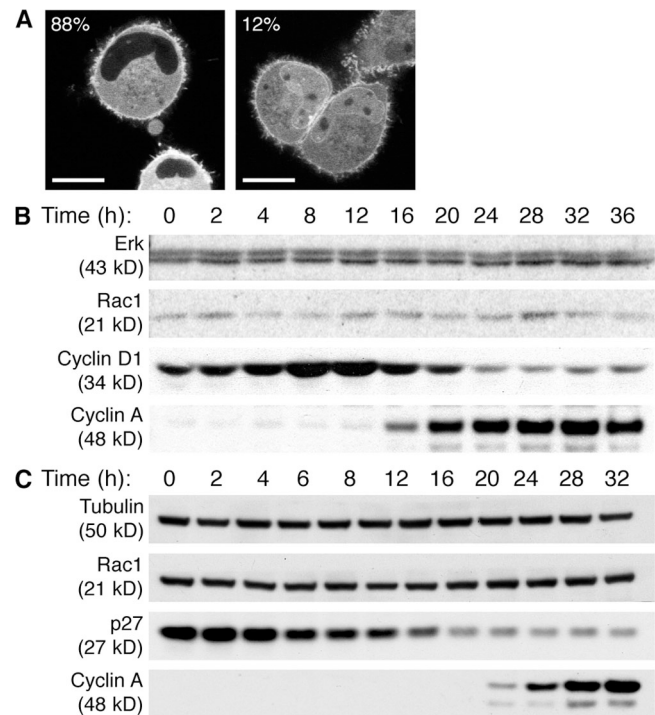


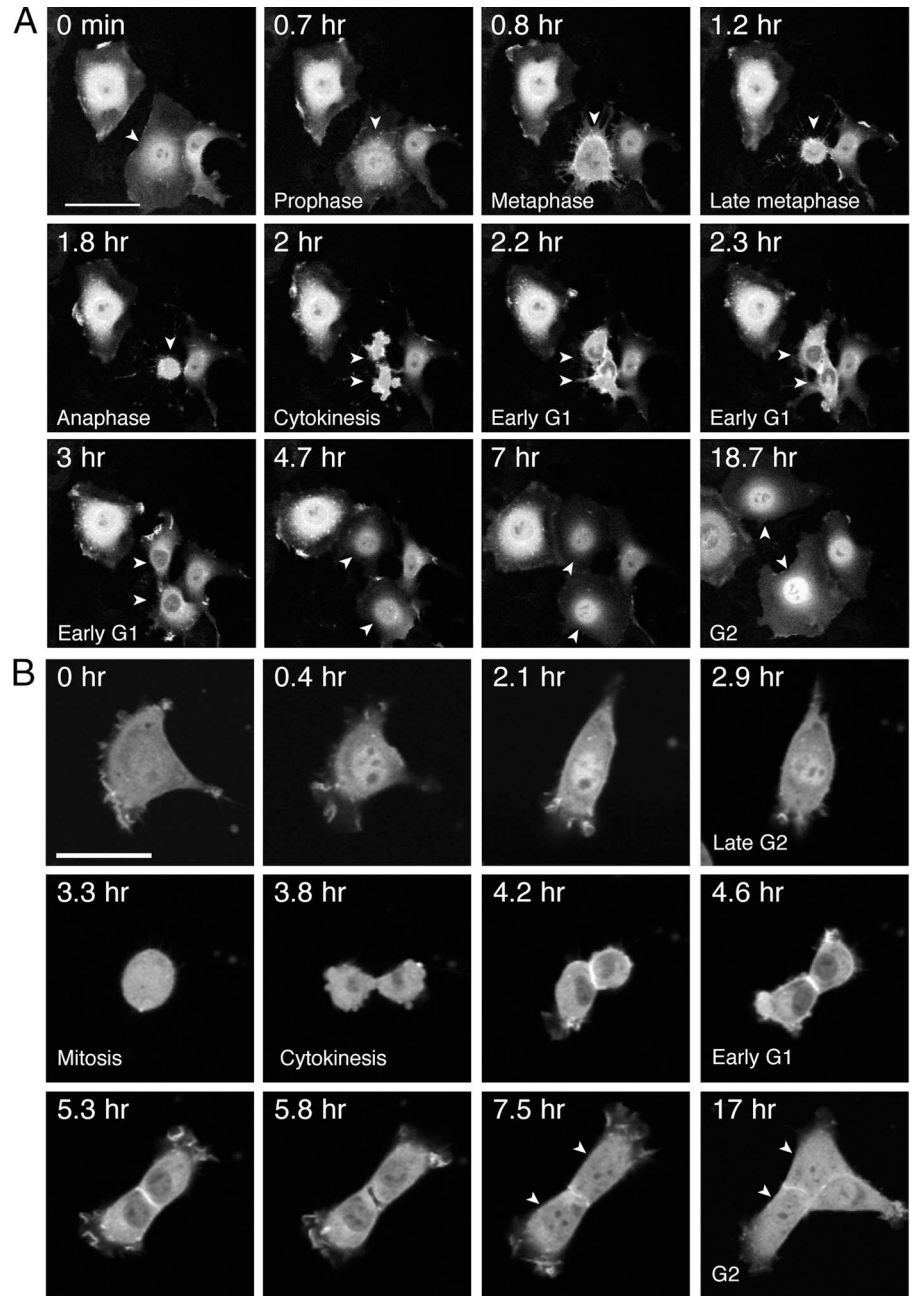
**Figure 6. Expression of Rac1 is constant through the cell cycle.** (A) Confocal images of asynchronous T98G cells expressing GFP-Rac1 with the percent of the transfected population represented by each pattern indicated. T98G (B) or IMR-90 (C) cells were synchronized by serum deprivation for 72 h and then induced to cycle by refeeding with 10% FBS. Aliquots of cells were harvested at the times indicated and assayed for Rac1 and the indicated control proteins by immunoblotting. Bar, 5  $\mu$ m.

GFP-Rac1 at levels below endogenous Rac1 (Fig. S2). In the majority of cells that we captured undergoing at least one round of cell division, we observed accumulation of GFP-Rac1 in the nuclei before mitosis and a dramatic exclusion of GFP-Rac1 in the nuclei of cells immediately after cytokinesis (Fig. 7 and Videos 1 and 2, available at <http://www.jcb.org/cgi/content/full/jcb.200801047/DC1>). Collectively, our data demonstrate a redistribution of Rac1 during the cell cycle, with the highest accumulation of Rac1 in the nucleus during G2.

#### Nuclear cycling of Rac1 promotes cell division

The accumulation of Rac1 in G2 suggested that nuclear Rac1 might play a role in cell division. To test this hypothesis, we studied cells that expressed GTP-bound forms of Rac1 capable of cycling in and out of the nucleus or restricted to one or the other compartment. Rac1L61 with a wild-type C terminus cycles in and out of the nucleus. Rac1L61 with the 14-amino acid C terminus of Kras4B substituted for the analogous Rac1 sequence (Rac1L61Ktail) was used to restrict the protein to the cytoplasm. Rac1L61 with the AAX residues of its CAAX motif removed (Rac1L61 $\Delta$ AAX) such that prenylation was blocked was used as a form that accumulated exclusively in the nucleus. GFP-tagged versions of these constructs were introduced into NIH 3T3 cells by retroviral transduction. Cytofluorimetry revealed that infection efficiency was high and that each population of infected cells expressed equivalent amounts

**Figure 7. Nuclear expression of Rac1 peaks in G2 in asynchronously dividing cells.** PAE (A) or NIH 3T3 (B) cells stably expressing GFP-Rac1 at levels below endogenous were examined by time-lapse confocal microscopy over one division cycle. Arrowheads indicate representative parent and daughter cells. Note that nuclear Rac1 is high immediately preceding mitosis and that GFP-Rac1 is excluded from the nuclei of the daughter cells immediately after cell division. See Videos 1 and 2 (available at <http://www.jcb.org/cgi/content/full/jcb.200801047/DC1>). Bars, 10  $\mu$ m.



of protein (Fig. 8 A). Confocal microscopy revealed that, as expected, although only a subset of GFP-Rac1L61-expressing cells showed nuclear fluorescence, each cell expressing GFP-Rac1L61 $\Delta$ AAX showed strong nuclear fluorescence (Fig. 8 B). Cells expressing GFP-Rac1L61Ktail showed no nuclear fluorescence, which is consistent with removal of the NLS (Fig. 8 B). Also as expected, differential interference contrast microscopy (not depicted) and phalloidin staining (Fig. 8 B) revealed that GFP-Rac1L61 promoted marked ruffling with prominent concentric lamellipodia. The phenotype of cells expressing GFP-Rac1L61Ktail was identical, which indicates that the ability of GTP-Rac1 to regulate actin remodeling was retained in the chimeric protein excluded from the nucleus and targeted to the plasma membrane with the K-Ras sequence. In contrast, cells expressing GFP-Rac1L61 $\Delta$ AAX did not show a ruffled pheno-

type, indicating that nuclear Rac1 cannot stimulate lamellipodia formation (Fig. 8 B).

Using time-lapse phase-contrast microscopy (Khodjakov and Rieder, 2006), we studied the mitotic index of the cells infected with the various constructs. GFP-Rac1L61 that is GTP-bound and capable of cycling in and out of the nucleus increased slightly the mitotic index (Fig. 8 C). In contrast, GFP-Rac1L61Ktail decreased the mitotic index, indicating that GTP-bound Rac1 restricted to the cytoplasm acts as a dominant negative with regard to the promotion of cell division. Importantly, GFP-Rac1L61 $\Delta$ AAX that was restricted to the nucleus significantly increased the mitotic index, which suggests that nuclear GTP-Rac1 promotes cell division. The activity of GFP-Rac1L61 $\Delta$ AAX in this assay prompted us to ask whether the Rac1 wild type at the GTP-binding domain could be loaded



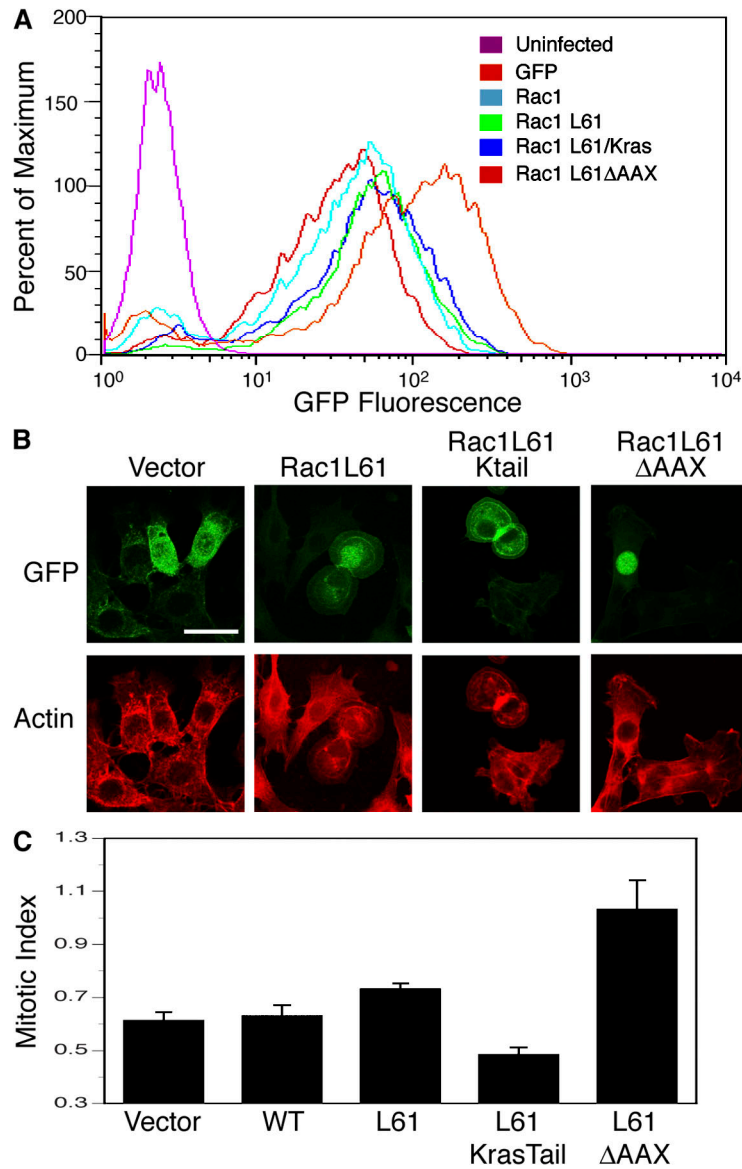


**Figure 8. Constitutive expression of activated Rac1 in the cytoplasm inhibits cell division and constitutive expression in the nucleus enhances cell division.** NIH 3T3 cells were transfected with the indicated constructs. Rac1L61/Ktail cannot enter the nucleus. Rac1L61ΔAAX is entirely nuclear. (A) Cytofluorimetry indicates equivalent expression levels. (B) TRITC-phalloidin staining reveals that although Rac1L61/Ktail induces marked peripheral ruffling like Rac1L61, Rac1L61ΔAAX does not. Bar, 10  $\mu$ m. (C) Mitotic index (mitoses per number of cells over 16 h) of cells transfected with the indicated constructs (mean  $\pm$  SEM;  $n = 3$ ).

with GTP when constitutively driven into the nucleus as a consequence of blocked prenylation. A GST-PAK-PBD pull-down assay revealed that GFP-Rac1ΔAAX and GFP-Rac1 were equivalently loaded with GTP when expressed at endogenous levels (Fig. S3, available at <http://www.jcb.org/cgi/content/full/jcb.200801047/DC1>), which suggests that at least a portion of the nuclear pool is activated.

## Discussion

Our data show that Rac1 possesses a strong but cryptic NLS. The NLS consists of the polybasic region of the C-terminal membrane-targeting domain and is strengthened by an adjacent triproline sequence. As such, it mimics the canonical NLS of polyomavirus large T antigen, which consists of a polybasic sequence preceded by a diproline (Chelsky et al., 1989). However, the strength of the NLS is greatly diminished by the geranylgeranyl lipid group that flanks the NLS on the C-terminal side. Although Rac1 is but one of many small GTPases with a polybasic

region that serves, along with a prenyl modification, as a plasma membrane-targeting motif (Hancock et al., 1990; Michaelson et al., 2001; Heo et al., 2006; Yeung et al., 2006), it is unique in serving as a strong NLS. The absence of a functional NLS in Rac2 (PPPVKKPGKK) or Rac1/Ktail (PPPKKKKKSKTK) suggests that an optimal charge distribution (+6) after a proline is required.

The inhibitory effect of the geranylgeranyl modification with regard to the NLS suggests that nuclear transport of Rac1 may be regulated by prenylation. However, prenylation is irreversible (Clarke, 1992), making any model that evokes deprenylation as the regulatory event for nuclear import untenable. Moreover, our observation that a significant pool of nuclear Rac1 remains prenylated demonstrates that nuclear entry does not require loss of the prenyl modification.

An alternative model would be sequestration of the geranylgeranyl group by a prenyl-binding protein that allows conditional engagement of importin- $\alpha$  by the NLS. RhoGDI binds geranylgeranylated Rac1 (Michaelson et al., 2001) and, by analogy

to the cocrystal of Cdc42 and RhoGDI, sequesters the geranylgeranyl group in a deep hydrophobic pocket (Hoffman et al., 2000). Exclusion of RhoGDI from the nucleus makes it an unlikely candidate for a chaperone that transits the nuclear pore, although it is conceivable that this chaperone could hand Rac1 off to importin- $\alpha$  on the cytoplasmic side of the nuclear pore complex. Indeed, the structure of a cocrystal of RhoGDI and Cdc42 shows the polybasic region adjacent to the buried geranylgeranyl group to lie on the solvent-exposed surface of the chaperone accessible to a potential ternary protein-protein interaction (Hoffman et al., 2000). GFP extended with the geranylgeranylated 21-amino acid tail of Rac1 cannot bind RhoGDI but entered the nucleus, demonstrating that RhoGDI binding is not required for nuclear import. However, this does not mean that RhoGDI does not play a role in sequestering Rac1 in the cytoplasm. In two out of three cell types tested, GFP extended with the 21-amino acid C terminus of Rac1 showed a frequency of nuclear localization almost as high as unprenylated GFP-Rac1SAAX. Thus, the geranylgeranylated construct that cannot bind RhoGDI resembles the nonprenylated protein, which suggests that RhoGDI plays a role in cytoplasmic retention.

The ability of the Rac1 polybasic region to bind to the inner leaflet of the plasma membrane and to serve as an NLS that binds to importin- $\alpha$  are likely mutually exclusive. In both cases, a simple model is one in which RhoGDI hands off Rac1 to either the plasma membrane or to importin- $\alpha$ . What regulates this decision could be yet-to-be identified GDI-releasing factors (Dirac-Svejstrup et al., 1997) that are coupled either to the plasma membrane or importin- $\alpha$ .

Although the C termini of small GTPases are the regions that vary the most through evolution, the NLS of Rac1 is highly conserved, which suggests a critical function. The fluctuation in nuclear Rac1 as cells proceed through their division cycle suggests that nuclear Rac1 plays a role in cell division. The entry of Rac1 into the nucleus before mitosis could function in two ways. The process could sequester Rac1 in the nucleus to diminish its effects in the cytoplasm, Rac1 could serve a specific function in the nucleoplasm, or both.

Radical changes to the cytoskeleton must accompany mitosis. In tissues, adherens junctions must break down. In monolayers, previously spread and adherent cells must detach from the substratum and round up. These are processes opposed by the biological actions of Rac1 on the cytoskeleton that promote ruffling, spreading, and adhesion (Takaishi et al., 1997; Jaffe and Hall, 2005). During cytokinesis, the cell must rapidly recover the ability to spread and adhere (Yoshizaki et al., 2003; Khodjakov and Rieder, 2006). Therefore, sequestration of Rac1 in the nucleus immediately before mitosis and release into the cytoplasm during cytokinesis would be an efficient way of accomplishing these tasks if the first line of control by GEFs and GAPs is not sufficient. The accumulation of one or more Rac1 GAPs in the nucleus might also play a role in this model. One candidate is MgcRacGAP, which is expressed in the nucleus (Hirose et al., 2001) and associates with the mitotic spindle, where aurora B kinase can alter its specificity toward Rac1 and Rho (Minoshima et al., 2003). Moreover, MgcRacGAP mRNA levels rise dramatically in G2 (Hirose et al., 2001), and the pro-

tein enters the nucleus in complex with Rac1 (Kawashima et al., 2006). Intriguingly, overexpression of dominant-negative forms of MgcRacGAP (Kawashima et al., 2000) as well as constitutively active Rac1V12 (Yoshizaki et al., 2004) led to multinucleate cells because of defects in cytokinesis, which suggests that inhibition of Rac1 by MgcRacGAP is required for cell division. Similar defects in cytokinesis were observed in *Caenorhabditis elegans* that harbored a temperature-sensitive allele of CYK-4 (Jantsch-Plunger et al., 2000), an orthologue of MgcRacGAP, which suggests that nuclear Rac1 GAP activity was necessary for cytokinesis. Our observation that GTP-bound Rac1 restricted to the cytoplasm with the C terminus of K-Ras4B results in diminished cell division supports a model whereby Rac1 must enter the nucleus in G2 and interact with MgcRacGAP to permit cytokinesis.

An alternative or additional model for the role of Rac1 in the nucleus is the regulation of a specific function or set of functions in that compartment during division. The numerous GEFs and GAPs that regulate Rac1 and the myriad of effectors regulated by Rac1 make such a model plausible. Although generally active at cell membranes as a consequence of their pleckstrin homology domains, Dbl domains containing Rho GEFs have been found in the nucleus (Rossman et al., 2005). Ect2 is a Rac1/Rho/Cdc42 GEF regulated by phosphorylation that occurs in G2 when it accumulates in the nucleoplasm (Tatsumoto et al., 1999), which is coincident with Rac1. The DOCK180-ELMO1 complex is a non-Dbl-containing GEF for Rac1 that is localized in the nucleus (Yin et al., 2004). Among Rac1 effectors, PAK1 and IQGAP2 have been described in the nucleus (Yamashiro et al., 2003; Singh et al., 2005). Rac1 is well known to regulate the transcription of certain genes (Jaffe and Hall, 2005). Although this activity could emanate from the cytoplasm, Rac1 could also have a more direct effect on the transcriptional machinery in the nucleus. Consistent with this idea is the observation that Rac1 interacts directly with STAT3 (Simon et al., 2000) and STAT5 (Kawashima et al., 2006). Also among the transcription factors regulated by Rac1 is nuclear factor  $\kappa$ B that, in turn, regulates expression of cyclin D1, which is critical for cell cycle progression (Hinze et al., 1999). Our observation that GTP-bound Rac1L61 $\Delta$ AAX, which is constitutively targeted to the nucleus, accelerates cell division, combined with our observation that at least a portion of wild-type Rac1 targeted to the nucleus in the same way is GTP-bound, supports a model in which nuclear Rac1 plays a positive role in the regulation of cell division.

## Materials and methods

### Cell culture, transfection, and infection

COS-1, ECV304, NIH3T3, T98G, IMR-90, and MDCK cells were obtained from the American Type Culture Collection. PAE cells were obtained from M. Klagsburn (Children's Hospital, Boston, MA). Phoenix retroviral producer cell lines were obtained from G. Nolan (Stanford University, Palo Alto, CA). Rac1flox/flox mouse embryonic fibroblasts were provided by V. Tybulewicz (National Institute for Medical Research, London, UK) and J. Kissel (Wistar Institute, Philadelphia, PA). Cells were grown in DME (Cellgro; Mediatech, Inc.) supplemented with glucose, L-glutamine, sodium pyruvate, 10% fetal bovine serum (for Cos-1, ECV 304, MDCK, T98G, IMR-90, and PAE; Cellgro), or 10% calf serum (for NIH 3T3 and Phoenix; Atlanta Biologicals) and antibiotics at 37°C and 5% CO<sub>2</sub>. For all high-magnification microscopy, cells were plated, transfected, and imaged in

the same 35-mm culture dish that incorporated a No. 1.5 glass coverslip-sealed 15-mm cut-out on the bottom (MatTek). Transfections were performed 1 d after plating at 50% confluence using SuperFect (QIAGEN) according to the manufacturer's instructions. Transiently transfected cells were analyzed 1 d after transfection. NIH 3T3 cells were infected as described previously (Pear et al., 1993). In brief, Phoenix cells plated on 60-mm dishes were cotransfected with the indicated MSCV-GFP plasmid and an ectopic helper vector using Superfect, with 3 ml of fresh media added 3 h after transfection. 27 and 50 h after transfection, 1 ml of cleared supernatant from the Phoenix cells was added to 2 ml of fresh media on NIH 3T3 cells in the presence of 5 µg/ml polybrene. PAE and ECV cells stably expressing GFP-Rac1 have been described previously (Michaelson et al., 2001). NIH 3T3 cells stably expressing GFP-Rac1 were derived by retroviral transduction with MSCV-GFP-Rac1 and selection in puromycin. Where indicated, cells were treated with 10 µM compactin for 24 h. Puromycin, compactin, and polybrene were obtained from Sigma-Aldrich.

#### Plasmids

Rac1, Rac1 L61, and Rac1-21aa (hypervariable domain of Rac1) were cloned into GFP-C3 (Clontech Laboratories, Inc.) to obtain the GFP fusion proteins as previously described (Michaelson et al., 2001). GFP fusion of Rac1 CVLS (farnesylated variant of Rac1) has also been described previously (Michaelson et al., 2005). The 11-amino acid hypervariable domain and the triple proline to alanine mutant version of the Rac1 hypervariable domain were generated using synthetic primers incorporating restriction enzyme sites for cloning into an EGFP-C3 vector (Clontech Laboratories, Inc.). Prenyl-deficient (GFP-C3-Rac1 SAAX and GFP-C3-Rac1 L61 SAAX) mutants were derived using QuikChange (Stratagene) site-directed mutagenesis of wild-type Rac1 or Rac1 L61. The GFP-C3-Rac1 L61/KRas construct was made using synthetic primers to replace the C-terminal 11 amino acids of Rac1 with the C-terminal 14 amino acids of K-Ras encoding the polybasic region. MSCV-GFP, MSCV-GFP-Rac1 L61, and MSCV-GFP-Rac1 L61 ΔAAX were generated from MSCV-GFP-Rac1 (provided by M. Dinauer, Indiana University School of Medicine, Indianapolis, IN) using QuikChange. Rac1 L61/KTail was digested from GFP-C3-Rac1 L61/KTail using BglII and ApaI (Roche) and used to replace Rac1 in the MSCV vector.

#### Fluorescence microscopy

Live cells were examined for CFP-, YFP-, or GFP-tagged proteins 24 h after transfection with an inverted epifluorescence microscope (Axiovert 100; Carl Zeiss, Inc.) with a 63× Plan-Apochromat 1.4 NA oil immersion objective equipped with a cooled charge-coupled device (CCD) camera (Princeton Instruments) and MetaMorph digital imaging software (MDS Analytical Technologies) or a laser scanning confocal microscope (510; Carl Zeiss, Inc.) incorporating an Axiovert 200M with the same objective. Time-lapse phase-contrast microscopy of dividing cells was performed with an inverted microscope (Axiovert 200; Carl Zeiss, Inc.) with a 10× Plan-Neofluar, 0.30 NA dry objective equipped with a cooled CCD camera (Retiga EX; QImaging) and acquisition software (OpenLab 3.1.7; Improvision). Living cells were imaged in 35-mm dishes (MatTek) either at room temperature or at 37°C with 5% CO<sub>2</sub> and humidified air using a metabolic chamber (PeCon). Digital images were processed for levels and gamma adjustment with Photoshop CS2 (Adobe). Nuclear localization of GFP-Rac1 constructs was determined by counting 50 or more cells per condition and scoring cells that had nuclear fluorescence stronger than surrounding cytoplasm.

#### Antibodies

Commercial antibodies used were anti-Rac1 monoclonal Ab (BD Biosciences or Millipore); anti-Rac1 polyclonal, anti-RhoA, -RhoB, -RCC1, -c-myc, -HDAC1, -HDAC3, -lamin A, -Erk 1, -cyclin A, and -RhoGDI antisera (Santa Cruz Biotechnology); lamin A (Cell Signaling Technology); lamin B (EMD); and anti-Ras10 monoclonal Ab (Millipore). Anti-Ran antisera were a gift of M. Rush (New York University School of Medicine, New York, NY). Texas Red-conjugated donkey anti-rabbit or rabbit anti-mouse were obtained from Jackson ImmunoResearch Laboratories.

#### Nuclear fractionation

Cells were grown to confluence in 10-cm plates and scraped into 500 µl RSB (10 mM Tris, pH 7.4, 10 mM NaCl, 3 mM MgCl<sub>2</sub>, and protease inhibitors), transferred to an Eppendorf tube, and centrifuged at a low speed (3,000 rpm for 1 min). The pellet was resuspended in 100 µl RSB-G40 (RSB with 10% glycerol and 0.25% NP-40) with 1 mM DTT and protease inhibitors and then centrifuged at 10,000 rpm for 1 min. The supernatant was saved as nonnuclear fraction and the pellet was rinsed once in RSB-

G40 and once in RSB-G (RSB with 10% glycerol). The final pellet was resuspended in 100 µl RSB-G40 as the nuclear fraction and 100 µl 2× SDS-PAGE buffer was added to both fractions. The nuclear fraction was sonicated to break up the DNA and equal volumes (equal cell equivalents) of both fractions were analyzed by SDS-PAGE and immunoblotting for a variety of nuclear and nonnuclear proteins. Proteins were detected and quantified using [<sup>125</sup>I]protein A and phosphorimaging.

#### Triton X-114 partitioning

Cells were partitioned using Triton X-114 as described previously (Hancock, 1995), with modifications. Four 10-cm plates of COS-1 cells at 50% confluency were scraped in PBS supplemented with 0.1% MgCl<sub>2</sub> and resuspended in 700 µl RSB. Precleared 10% Triton X-114 was added to 0.1% and incubated for 15 min. Lysates were centrifuged at 1,300 g and the nonnuclear fraction was separated from pelleted nuclei. Nuclei were resuspended in an equivalent amount of RSB and both the nuclear and nonnuclear fractions were supplemented with Triton X-114 to 1%. Nuclei were broken using seven cycles of 5-s sonication followed by 55 s on ice. Both fractions were centrifuged at full speed at 4°C to pellet any cellular debris. Supernatants were partitioned by incubating at 37° for 5 min and the now turbid fractions were centrifuged at full speed for 2 min at room temperature. The upper aqueous phase was carefully separated into a fresh tube and any remaining aqueous phase was removed. RSB was added to the detergent phase and 10% Triton X-114 was added to the aqueous phase to bring the two partitions to equivalent detergent concentration. SDS sample buffer was then added to the partitioned fractions, which were analyzed by SDS-PAGE and immunoblotting. Proteins were detected and quantified with [<sup>125</sup>I]protein A and phosphorimaging.

#### Cell cycle blocks

The cell cycle inhibitors 5-fluorouracil, daidzein, apigenin, olomoucine, and hydroxyurea were obtained from Sigma-Aldrich. Cells stably expressing GFP-Rac1 were treated with various concentrations of these agents for 24 h. For synchronization, cells were first blocked in G<sub>0</sub> by serum starvation for 24 h and released into medium containing 10% serum and 6 mM hydroxyurea for 24 h to block in S phase. Cells were then released from the block by transferring to standard growth medium and monitored by microscopy to determine changes in nuclear localization. The cell cycle distribution of cells in culture was determined by propidium iodide (Invitrogen) analysis of DNA content by cytofluorimetry. T98G and IMR-90 cells were blocked at G<sub>0</sub> by serum starvation (0.2% FCS for 3 d) and released by transfer to DME with 10% FBS. Lysates were prepared at various times with lysis buffer (50 mM Tris, pH 7.5, 250 mM NaCl, 0.1% Triton X-100, 1 mM EDTA, protease inhibitors, and phosphatase inhibitors) and analyzed by immunoblotting.

#### Phalloidin staining

Cells grown on 12-mm coverslips were transfected with GFP fusion constructs and fixed (3.7% paraformaldehyde) and permeabilized (0.1% Triton X-100) 24 h later. Cells were stained with 28 nM rhodamine phalloidin (Cytoskeleton, Inc.).

#### Mitotic index

48 h after retroviral infection, NIH 3T3 cells were plated sparsely on a 60-mm dish, and ~25 cells in a single field (10× objective) were imaged by time-lapse phase-contrast microscopy (1 frame every 5 min) using a metabolic chamber. Cell divisions were counted manually and the mitotic index was determined as a ratio of the number of divisions over 16 h divided by the number of cells in the starting frame.

#### Online supplemental material

Fig. S1 shows that commercial anti-Rac1 antibodies are not Rac1-specific in indirect IF staining. Fig. S2 shows relative expression of GFP-tagged Rac1 and endogenous Rac1 in stably transduced cells. Fig. S3 shows that nuclear Rac1 can be loaded with GTP. Video 1 shows that Rac1 accumulates in the nucleus of PAE cells before mitosis (G2) and is excluded afterward (G1). Video 2 shows that Rac1 accumulates in the nucleus of NIH 3T3 cells before mitosis (G2) and is excluded afterward (G1). Online supplemental material is available at <http://www.jcb.org/cgi/content/full/jcb.200801047/DC1>.

This work was supported by grants from the National Institutes of Health (CA116034, CA118495, and GM55279 to M.R. Philips and R37-CA76584, R01-GM57587, and R21-CA125173 to M. Pagano) and the New York State Department of Health Breast Cancer Research and Education Program (to M.R. Philips and D. Michaelson).

Submitted: 9 January 2008

Accepted: 1 April 2008

## References

- Chan, A.Y., S.J. Coniglio, Y.Y. Chuang, D. Michaelson, U.G. Knaus, M.R. Philips, and M. Symons. 2005. Roles of the Rac1 and Rac3 GTPases in human tumor cell invasion. *Oncogene*. 24:7821–7829.
- Chelsky, D., R. Ralph, and G. Jonak. 1989. Sequence requirements for synthetic peptide-mediated translocation to the nucleus. *Mol. Cell. Biol.* 9:2487–2492.
- Clarke, S. 1992. Protein isoprenylation and methylation at carboxyl-terminal cysteine residues. *Annu. Rev. Biochem.* 61:355–386.
- Dirac-Svejstrup, A.B., T. Sumizawa, and S.R. Pfeffer. 1997. Identification of a GDI displacement factor that releases endosomal Rab GTPases from Rab-GDI. *EMBO J.* 16:465–472.
- Dorrello, N.V., A. Peschiaroli, D. Guardavaccaro, N.H. Colburn, N.E. Sherman, and M. Pagano. 2006. S6K1- and betaTRCP-mediated degradation of PDCD4 promotes protein translation and cell growth. *Science*. 314:467–471.
- Hancock, J.F. 1995. Prenylation and palmitoylation analysis. *Methods Enzymol.* 255:237–245.
- Hancock, J.F., H. Paterson, and C.J. Marshall. 1990. A polybasic domain or palmitoylation is required in addition to the CAAX motif to localize p21<sup>ras</sup> to the plasma membrane. *Cell*. 63:133–139.
- Heo, W.D., T. Inoue, W.S. Park, M.L. Kim, B.O. Park, T.J. Wandless, and T. Meyer. 2006. PI(3,4,5)P3 and PI(4,5)P2 lipids target proteins with polybasic clusters to the plasma membrane. *Science*. 314:1458–1461.
- Hinz, M., D. Krappmann, A. Eichten, A. Heder, C. Scheidereit, and M. Strauss. 1999. NF-kappaB function in growth control: regulation of cyclin D1 expression and G0/G1-to-S-phase transition. *Mol. Cell. Biol.* 19:2690–2698.
- Hirose, K., T. Kawashima, I. Iwamoto, T. Nosaka, and T. Kitamura. 2001. MgcRacGAP is involved in cytokinesis through associating with mitotic spindle and midbody. *J. Biol. Chem.* 276:5821–5828.
- Hoffman, G.R., N. Nassar, and R.A. Cerione. 2000. Structure of the Rho family GTP-binding protein Cdc42 in complex with the multifunctional regulator RhoGDI. *Cell*. 100:345–356.
- Jaffe, A.B., and A. Hall. 2005. Rho GTPases: biochemistry and biology. *Annu. Rev. Cell Dev. Biol.* 21:247–269.
- Jantsch-Plunger, V., P. Gonczy, A. Romano, H. Schnabel, D. Hamill, R. Schnabel, A.A. Hyman, and M. Glotzer. 2000. CYK-4: A Rho family GTPase activating protein (GAP) required for central spindle formation and cytokinesis. *J. Cell Biol.* 149:1391–1404.
- Kawashima, T., K. Hirose, T. Satoh, A. Kaneko, Y. Ikeda, Y. Kaziro, T. Nosaka, and T. Kitamura. 2000. MgcRacGAP is involved in the control of growth and differentiation of hematopoietic cells. *Blood*. 96:2116–2124.
- Kawashima, T., Y.C. Bao, Y. Nomura, Y. Moon, Y. Tonozuka, Y. Minoshima, T. Hatori, A. Tsuchiya, M. Kiyono, T. Nosaka, et al. 2006. Rac1 and a GTPase-activating protein, MgcRacGAP, are required for nuclear translocation of STAT transcription factors. *J. Cell Biol.* 175:937–946.
- Khodjakov, A., and C.L. Rieder. 2006. Imaging the division process in living tissue culture cells. *Methods*. 38:2–16.
- Kitten, G.T., and E.A. Nigg. 1991. The CaaX motif is required for isoprenylation, carboxyl methylation, and nuclear membrane association of lamin B2. *J. Cell Biol.* 113:13–23.
- Kraynov, V.S., C. Chamberlain, G.M. Bokoch, M.A. Schwartz, S. Slabaugh, and K.M. Hahn. 2000. Localized Rac activation dynamics visualized in living cells. *Science*. 290:333–337.
- Lanning, C.C., R. Ruiz-Velasco, and C.L. Williams. 2003. Novel mechanism of the co-regulation of nuclear transport of SmgGDS and Rac1. *J. Biol. Chem.* 278:12495–12506.
- Lanning, C.C., J.L. Daddona, R. Ruiz-Velasco, S.H. Shafer, and C.L. Williams. 2004. The Rac1 C-terminal polybasic region regulates the nuclear localization and protein degradation of Rac1. *J. Biol. Chem.* 279:44197–44210.
- Michaelson, D., J. Silletti, G. Murphy, P. D'Eustachio, M. Rush, and M.R. Philips. 2001. Differential localization of Rho GTPases in live cells. Regulation by hypervariable regions and rhogdi binding. *J. Cell Biol.* 152:111–126.
- Michaelson, D., W. Ali, V.K. Chiu, M. Bergo, J. Silletti, L. Wright, S.G. Young, and M. Philips. 2005. Postprenylation CAAX processing is required for proper localization of Ras but not Rho GTPases. *Mol. Biol. Cell.* 16:1606–1616.
- Minoshima, Y., T. Kawashima, K. Hirose, Y. Tonozuka, A. Kawajiri, Y.C. Bao, X. Deng, M. Tatsuka, S. Narumiya, W.S. May Jr., et al. 2003. Phosphorylation by aurora B converts MgcRacGAP to a RhoGAP during cytokinesis. *Dev. Cell*. 4:549–560.
- Mor, A., and M.R. Philips. 2006. Compartmentalized Ras/MAPK signaling. *Annu. Rev. Immunol.* 24:771–800.
- Pear, W.S., G.P. Nolan, M.L. Scott, and D. Baltimore. 1993. Production of high-titer helper-free retroviruses by transient transfection. *Proc. Natl. Acad. Sci. USA*. 90:8392–8396.
- Plaumann, B., M. Fritsche, H. Rimpler, G. Brandner, and R.D. Hess. 1996. Flavonoids activate wild-type p53. *Oncogene*. 13:1605–1614.
- Rossman, K.L., C.J. Der, and J. Sondek. 2005. GEF means go: turning on RHO GTPases with guanine nucleotide-exchange factors. *Nat. Rev. Mol. Cell Biol.* 6:167–180.
- Sherwood, S.W., D. Rush, J.L. Ellsworth, and R.T. Schimke. 1988. Defining cellular senescence in IMR-90 cells: a flow cytometric analysis. *Proc. Natl. Acad. Sci. USA*. 85:9086–9090.
- Simon, A.R., H.G. Vikis, S. Stewart, B.L. Fanburg, B.H. Cochran, and K.L. Guan. 2000. Regulation of STAT3 by direct binding to the rac1 GTPase. *Science*. 290:144–147.
- Singh, R.R., C. Song, Z. Yang, and R. Kumar. 2005. Nuclear localization and chromatin targets of p21-activated kinase 1. *J. Biol. Chem.* 280:18130–18137.
- Takaishi, K., T. Sasaki, H. Kotani, H. Nishioka, and Y. Takai. 1997. Regulation of cell-cell adhesion by rac and rho small G proteins in MDCK cells. *J. Cell Biol.* 139:1047–1059.
- Tatsumoto, T., X. Xie, R. Blumenthal, I. Okamoto, and T. Miki. 1999. Human ECT2 is an exchange factor for Rho GTPases, phosphorylated in G2/M phases, and involved in cytokinesis. *J. Cell Biol.* 147:921–928.
- Walmsley, M.J., S.K. Ooi, L.F. Reynolds, S.H. Smith, S. Ruf, A. Mathiot, L. Vanes, D.A. Williams, M.P. Cancro, and V.L. Tybulewicz. 2003. Critical roles for Rac1 and Rac2 GTPases in B cell development and signaling. *Science*. 302:459–462.
- Westwick, J.K., Q.T. Lambert, G.J. Clark, M. Symons, L. Van Aelst, R.G. Pestell, and C.J. Der. 1997. Rac regulation of transformation, gene expression, and actin organization by multiple, PAK-independent pathways. *Mol. Cell. Biol.* 17:1324–1335.
- Wong, K.W., and R.R. Isberg. 2005. *Yersinia pseudotuberculosis* spatially controls activation and misregulation of host cell Rac1. *PLoS Pathog.* 1:e16.
- Yamashiro, S., T. Noguchi, and I. Mabuchi. 2003. Localization of two IQGAPs in cultured cells and early embryos of *Xenopus laevis*. *Cell Motil. Cytoskeleton*. 55:36–50.
- Yeung, T., M. Terebiznik, L. Yu, J. Silvius, W.M. Abidi, M. Philips, T. Levine, A. Kapus, and S. Grinstein. 2006. Receptor activation alters inner surface potential during phagocytosis. *Science*. 313:347–351.
- Yin, J., L. Haney, S. Zhou, K.S. Ravichandran, and W. Wang. 2004. Nuclear localization of the DOCK180/ELMO complex. *Arch. Biochem. Biophys.* 429:23–29.
- Yoshizaki, H., Y. Ohba, K. Kurokawa, R.E. Itoh, T. Nakamura, N. Mochizuki, K. Nagashima, and M. Matsuda. 2003. Activity of Rho-family GTPases during cell division as visualized with FRET-based probes. *J. Cell Biol.* 162:223–232.
- Yoshizaki, H., Y. Ohba, M.C. Parrini, N.G. Dulyaninova, A.R. Bresnick, N. Mochizuki, and M. Matsuda. 2004. Cell type-specific regulation of RhoA activity during cytokinesis. *J. Biol. Chem.* 279:44756–44762.